Physics, Chemistry, and Dynamics of Interplanetary Dust
ASP Conference Series, Vol. 104, 1996
Bo A. S. Gustafson and Martha S. Hanner (eds.)

Radial Velocities of Dust Particles in the F-Corona

L.I. Shestakova, A.K. Aimanov and G.K. Aimanova
Fesenkov Astrophysical Institute, 480068, Almaty, Kazakstan

Abstract. Observations of radial velocities in the F-corona in the elongation range from 3 to 6 solar radii were carried out on July 11, 1991 (Mexico, La Paz) by means of a Fabry-Perot spectrograph. The Fraunhofer lines in the spectral region of H and K CaII were used. The average velocities to the West and to the East of the Sun within 30° of the ecliptic plane are +30 km/s and -27 km/s respectively. This confirms the main results of the F-corona radial velocity observations by Shcheglov et al. (1987), Shestakova (1987) on July 31, 1981 about predominance of prograde Keplerian motion of the dust near the ecliptic plane and the effective radius of dust grains (≈0.4μm).

Introduction

Observations of the radial velocity field in the F-corona on July 31, 1981 (Shcheglov et al. 1987, Shestakova 1987) permitted us to obtain a two-dimensional distribution of the dust radial velocity in the elongation range from 3 to 7 solar radii ($r_\odot$). To analyze the results obtained near the ecliptic plane we suggested an undisturbed distribution of the dust grain concentration depending on the heliocentric distance according to the law $n(r) = n_0 r^{-\nu}$ for $r > r_0$ where r_0 is the radius of the dust free zone (DFZ) near the Sun.

Calculations showed that model parameters $\nu = 1.1$, $r_0 = 6.5\, r_\odot$ and the mean size of dust grains $\overline{s} = 0.4\mu m$ satisfied these observations. Observed projections of the velocities on the line-of-sight (LS) coincide with the Keplerian dust motion at a distance near 15 $r_\odot$. We showed that beyond this distance a new rise of the concentration n_0 cannot exist in addition to the undisturbed power law. Regions of enhanced dust concentration can exist in the distance range from 6.5 to 15 $r_\odot$. During the total solar eclipse in July 11, 1991 we tried to repeat this experiment.

Observations

The observational method is described by Aimanov et al. (1995). The center of the interference rings coincided with that of the Sun's image. The Doppler shifts were measured relative to identical Fraunhofer features of the day sky spectrum, obtained just after the total phase. We used several radial scans with the position angles shown in Fig. 1. The Doppler shifts were obtained along each measured scan at the points of intersections with Fraunhofer rings. The results averaged with two methods are presented in Figs. 1 and 2. Fig. 1 shows a dependence of the mean radial velocity on the position angle. It is seen that in the East direction velocities are negative and positive in the West direction. This confirms the existence of dust moving on Keplerian orbits in the prograde direction. Fig. 2 gives a mean dependence of the radial velocities on elongations. Points are obtained by averaging in the range of ±30° near the ecliptic plane. The West (W), East (E) and mean (W-E) directions are given separately.

Discussion

According to Shestakova (1987) observations of the velocity in the F-corona are presented as the average weighted over the brightness in the form of an integral along the line of sight

$$V(\epsilon) = \frac{\mu V_E}{\sin^{1/2}\epsilon} \frac{\int_\epsilon^\pi \sin^{\nu+3/2}\theta\sigma(\theta)d\theta}{\int_\epsilon^\pi \sin^\nu \theta\sigma(\theta)d\theta}, \tag{1}$$

where

$$\sigma(\theta) = s^2[A/4 + \frac{J_1^2(\kappa\sin\theta)}{\sin^2\theta}]$$

is a function of diffraction scattering, ϵ and θ are the elongation and scattering angle respectively, V_E is the orbital velocity of the Earth, $\mu = (1-\beta)^{1/2}$ is a coefficient taking into account the effect of radiation pressure, β is the ratio of radiation pressure to gravity, s is the grain radius, A is albedo, $\kappa = 2\pi s/\lambda$ is the size parameter, J_1^2 is a Bessel function. Since observations were made through the DFZ each integral in Eq.(1) is divided into two parts with the following limits: the first one from ϵ to θ_0, the second one from $\pi - \theta_0$ to π, where $\theta_0 = \arcsin(R_0 \sin\epsilon/r_0)$ and $R_0 = 1$ AU. In Fig. 3 we present results of the numerical calculation of the radial velocity (Eq. (1)) with parameters $\nu = 1.1$, $\bar{s} = 0.45$ µm and $r_0 = 7\, r_\odot$ giving good agreement with both observations. For comparison we give the observational results obtained in 1981 (Shestakova 1987) and in 1991 (Aimanov et al. 1995).

When $\nu = 1$ an analytical solution of Eq.(1) is possible in the elongation range $R_0\,\epsilon < 0.7\, r_0$

$$V(\epsilon) = \frac{4\mu V_E (R_0/r_0)^{1/2}}{\pi\bar{\kappa}}, \tag{2}$$

where $\bar{\kappa}$ is a mean effective size parameter. Use of Eq.(2) means a fulfillment of two conditions: $\bar{\kappa}\theta_0 >> 1$ (large grains) and $\bar{\kappa}\epsilon << 1$ (small angles). In fact for observations in the solar corona in the optical region this restriction means that Eq. (2) can be used when $0.2\mu m < \bar{s} < 3\mu m$. If one considers in Eq.(1) a more realistic scattering function, weighted over a grain size distribution in the form $n(s) = n_0\, s^{-p}$ then the analytical solution of Eq.(1) also can be obtained in some cases. For example, in the case p = 4 we obtain an expression like Eq.(2) where instead of $\bar{\kappa}$ will be $2\kappa_1$, κ_1 is the lower limit of this parameter corresponding to the lower limit of the grain size s_1. From Eq.(2) it follows that $\bar{s} \approx 0.5\mu m$ (or $s_1 \sim 0.2\mu m$), close to the results of our numerical calculations. In Fig. 3 we present results of numerical calculations of the radial velocity (Eq. (1)) with $\nu = 1.1$, $s_1 = 0.45\mu m$ and $r_0 = 7\, r_\odot$, giving good agreement with the 1981 observations. Eq. (2) corresponds to the inner flat part of the curve in Fig. 3.

In order to compare the results of the different methods to observe the F-corona, it is necessary to consider the weighting function looking like $\sin^\alpha\theta$ in the corresponding integrals. We have $\sin^{\nu+3/2}\theta$ for the method of radial velocities, $\sin^\nu\theta$ for the brightness integral and $\sin^{\nu-2}\theta$ in the expression of the thermal emission integral. One can see that $\sin^{\nu+3/2}\theta$ distinguishes most effectively the contribution of the coronal region where

https://doi.org/10.1017/S025292110050181X Published online by Cambridge University Press

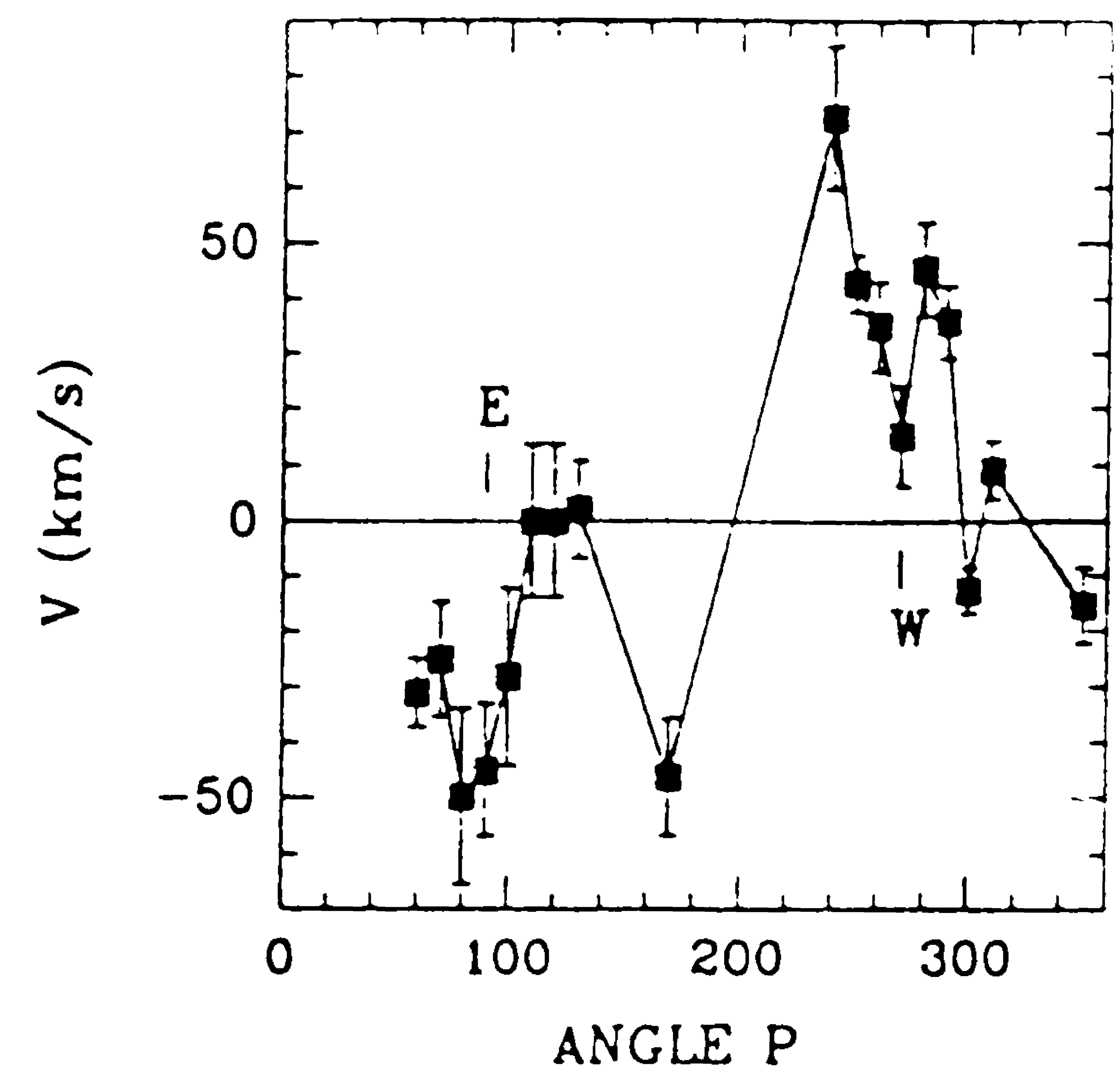

Fig. 1 Observed radial velocities depending on the position angle. Points are obtained by averaging over elongations in the range (3 - 5)$r_\odot$. The beginning of the account 0° is in the direction to the North pole of the ecliptic.

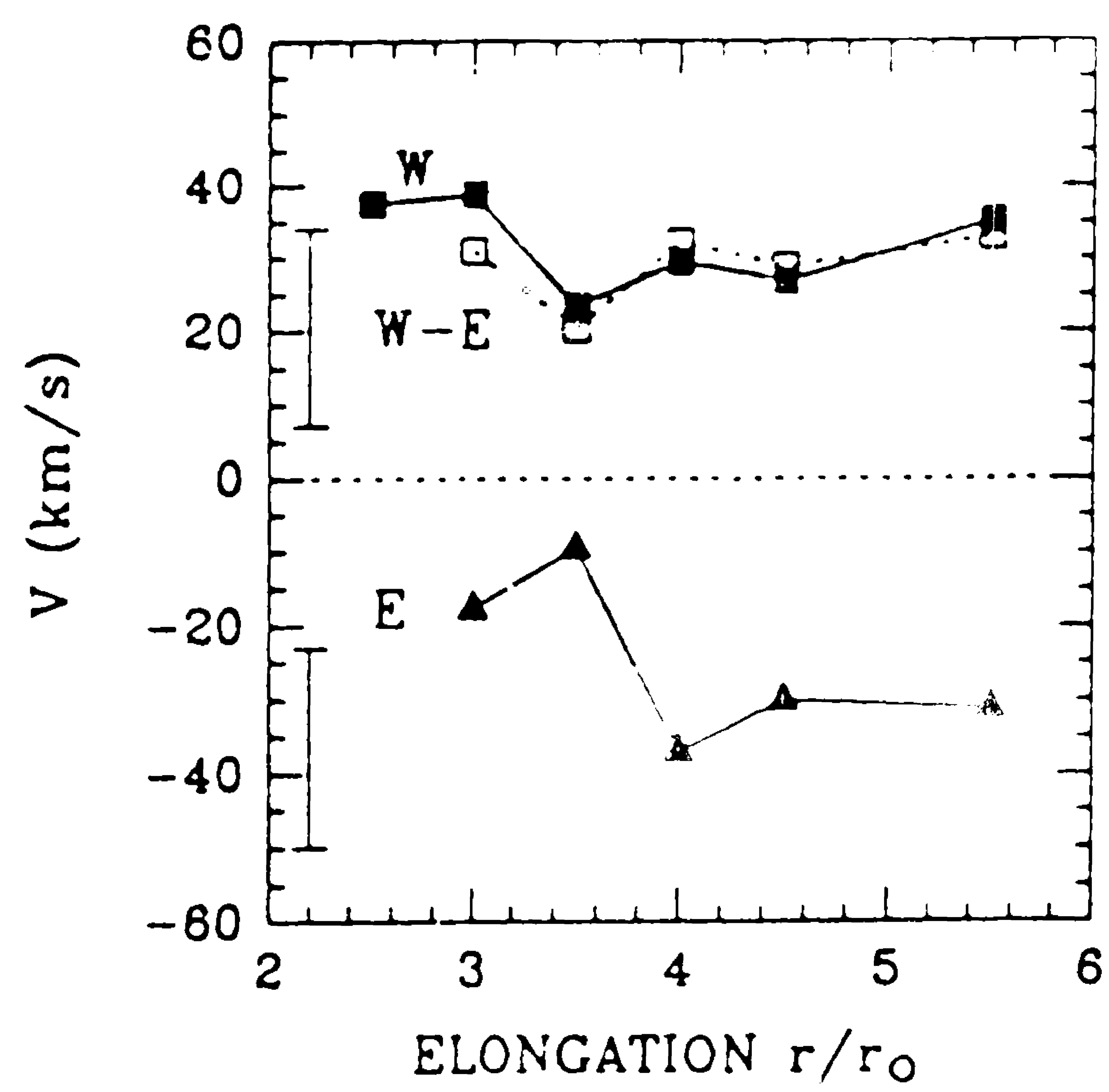

Fig. 2 Mean radial velocities near the ecliptic plane (±30°) as a function of the elongation. The range of averaging over the elongation is 0.5 $r_\odot$.

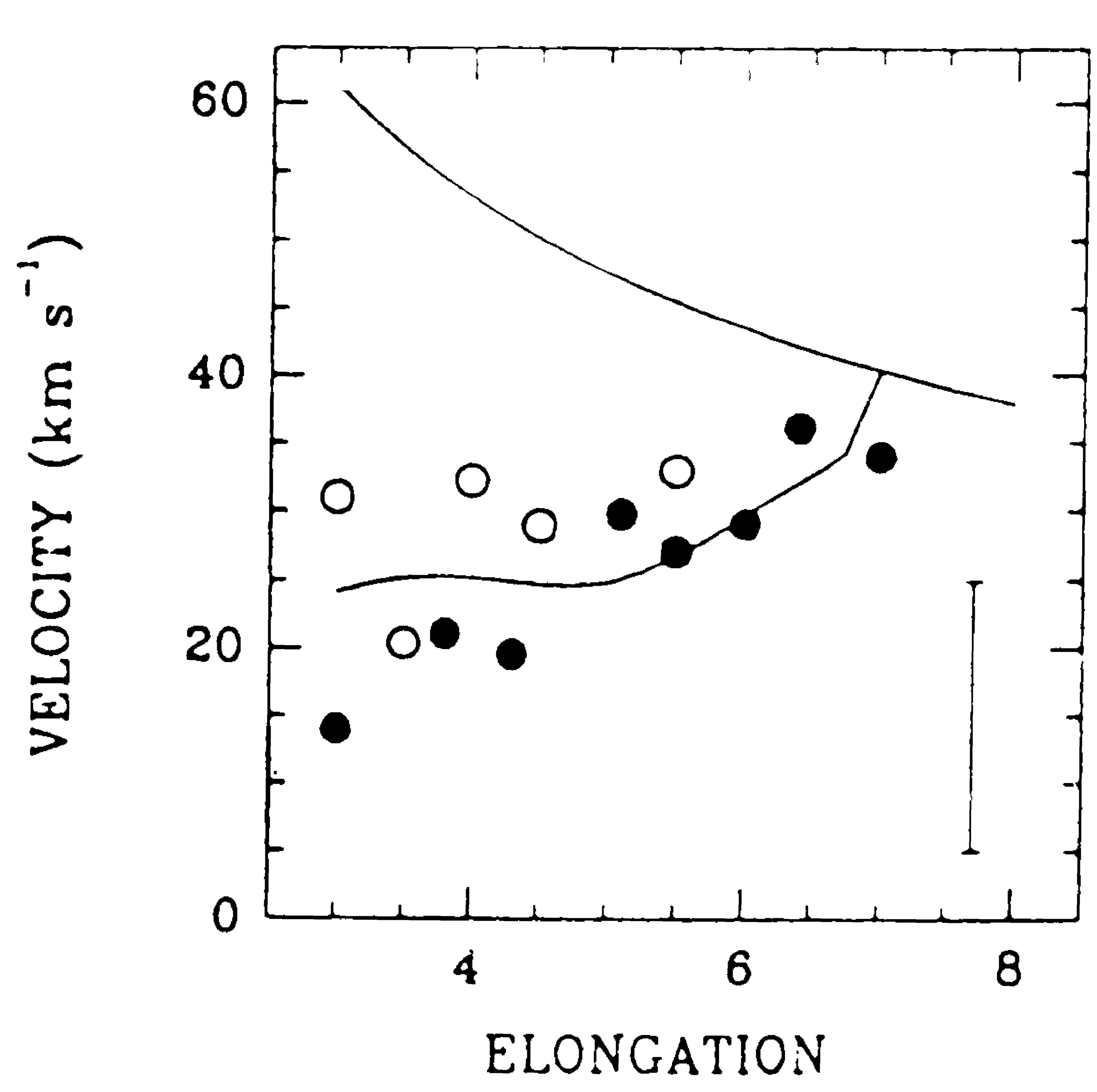

Fig. 3 Calculated radial velocities versus elongations in solar radii. Parameters: $\nu = 1.1$, the radius of the grain $s = 0.45$ μm, $A = 0.25$. Upper solid line is the case when a dust free zone (DFZ) is absent; lower one when the radius of DFZ equals 7 $r_\odot$. *Full* circles are observations of 1981, *open* circles are those of 1991.

$\theta \approx 90°$; thus, the dependence of the results on the choice of the model is minimal. Moreover, there exists direct evidence that the results refer to the region of the F-corona: 1) projections of the circular velocities on the line of sight for the particles beyond 17 $r_\odot$ are less than those we measured during two eclipses; 2) the more precise and complete data on radial velocities in the corona in 1981 definitely point to the growth of the observed velocity with elongation. This is possible if we observe through the DFZ; beyond this zone the Keplerian law $V \sim 1/\sqrt{r}$ has to be realized (Fig. 3).

Suggesting the undisturbed distribution of the dust concentration according to the law $n(r) \sim r^{-\nu}$ in the observed range of distances 6.5 $r_\odot < r <$ 17 $r_\odot$, we found that the main contribution to scattering is made by the grains with s = 0.4 - 0.5 μm, that is, 1 - 2 orders of magnitude less than those of the Zodiacal Cloud. The size values may be changed if an excess concentration will be detected in the distance range mentioned above.

The existence of such a large DFZ for the usual Zodiacal dust does not exclude penetration of large comet-like bodies, whose remnants can reach 4.0 - 4.3 $r_\odot$. The second possibility to increase the contribution of the corona to the brightness along the line of sight is to change the scattering function $\sigma(\theta,\kappa)$. When observing in the near IR region, the parameter κ decreases because λ increases. This is equivalent to increasing the contribution of smaller grains in the VSF The IR observations of the F-corona in 1991 (Lamy et al. 1992; Mann and MacQueen, 1993) showed that for small elongations the observed intensity was significantly higher than that due to scattering with use of the VSF in the visible region. We favor the model with undisturbed dust distribution up to the DFZ as more reliable because of the absence of the thermal emission in the corona in 1991 (Hodapp et al. 1992; Lamy et al. 1992). An excess of small dust grains in the F-corona, invisible in observations of the brightness but seen with the radial velocity method, is confirmed by our calculations (Shestakova and Tambovtseva, 1995).

References

Aimanov A.K., Aimanova G.K., Shestakova L.I., 1995, Astron. Letters **21**, 196

Hodapp K.-W., MacQueen R.M., Hall D.N.B., 1992, Nat., **335**, 707

Lamy P.L., Kuhn J.R., Lin H., Koutchmy S., Smartt R.N., 1992, Sci., **257**, 1377

Mann I. and MacQueen R. M., 1993, A&A **275**, 293

Shcheglov P.V., Shestakova L.I., Aimanov A.K., 1987, A&A, **173**, 383

Shestakova L.I., 1987, A&A, **175**, 289

Shestakova L. I., Tambovtseva L. V., 1995, Astron. Astrophys. Trans. **8**, 59